Measurement of Compton Scattering from the Deuteron and an Improved Extraction of the Neutron Electromagnetic Polarizabilities

L. S. Myers,[1,*] J. R. M. Annand,[2] J. Brudvik,[3] G. Feldman,[4] K. G. Fissum,[5,†] H. W. Grießhammer,[4] K. Hansen,[3] S. S. Henshaw,[6,‡] L. Isaksson,[3] R. Jebali,[2] M. A. Kovash,[7] M. Lundin,[3] J. A. McGovern,[8] D. G. Middleton,[9] A. M. Nathan,[1] D. R. Phillips,[10] B. Schröder,[3,5] and S. C. Stave[6,§]

(COMPTON@MAX-lab Collaboration)

[1]*Department of Physics, University of Illinois at Urbana-Champaign, Urbana, Illinois 61801, USA*
[2]*School of Physics and Astronomy, University of Glasgow, Glasgow G12 8QQ, Scotland, United Kingdom*
[3]*MAX IV Laboratory, Lund University, SE-221 00 Lund, Sweden*
[4]*Institute for Nuclear Studies, Department of Physics, The George Washington University, Washington, DC 20052, USA*
[5]*Department of Physics, Lund University, SE-221 00 Lund, Sweden*
[6]*Department of Physics, Duke University, Durham, North Carolina 27708, USA*
[7]*Department of Physics and Astronomy, University of Kentucky, Lexington, Kentucky 40506, USA*
[8]*School of Physics and Astronomy, The University of Manchester, Manchester M13 9PL, United Kingdom*
[9]*Kepler Centre for Astro- and Particle Physics, Physikalisches Institut, Universität Tübingen, D-72076 Tübingen, Germany*
[10]*Department of Physics and Astronomy and Institute of Nuclear and Particle Physics, Ohio University, Athens, Ohio 45701, USA*

(Received 19 September 2014; published 31 December 2014)

The electromagnetic polarizabilities of the nucleon are fundamental properties that describe its response to external electric and magnetic fields. They can be extracted from Compton-scattering data—and have been, with good accuracy, in the case of the proton. In contradistinction, information for the neutron requires the use of Compton scattering from nuclear targets. Here, we report a new measurement of elastic photon scattering from deuterium using quasimonoenergetic tagged photons at the MAX IV Laboratory in Lund, Sweden. These first new data in more than a decade effectively double the world data set. Their energy range overlaps with previous experiments and extends it by 20 MeV to higher energies. An analysis using chiral effective field theory with dynamical $\Delta(1232)$ degrees of freedom shows the data are consistent with and within the world data set. After demonstrating that the fit is consistent with the Baldin sum rule, extracting values for the isoscalar nucleon polarizabilities, and combining them with a recent result for the proton, we obtain the neutron polarizabilities as $\alpha_n = [11.55 \pm 1.25(\text{stat}) \pm 0.2(\text{BSR}) \pm 0.8(\text{th})] \times 10^{-4}$ fm^3 and $\beta_n = [3.65 \mp 1.25(\text{stat}) \pm 0.2(\text{BSR}) \mp 0.8(\text{th})] \times 10^{-4}$ fm^3, with $\chi^2 = 45.2$ for 44 degrees of freedom.

DOI: 10.1103/PhysRevLett.113.262506 PACS numbers: 25.20.Dc, 24.70.+s

The electric and magnetic dipole polarizabilities α and β of the proton and neutron have recently drawn much attention; see, e.g., Ref. [1] for a review and Ref. [2] for an open letter. They encode the response of the nucleon to applied electric or magnetic fields, and summarize information on the entire spectrum of nucleonic excitation, offering a stringent test of our understanding of quantum chromodynamics (QCD). Full lattice QCD results with realistic uncertainties are anticipated in the near future [3]. Besides being fundamental nucleon properties, α and β are relevant for theoretical studies of the Lamb shift of muonic hydrogen and of the proton-neutron mass difference, and dominate the uncertainties of both [4–7].

The majority of nucleon-polarizability measurements have used nuclear Compton scattering. This Letter reports new results for the deuteron, where elastic Compton scattering provides access to the isoscalar average of proton and neutron polarizabilities α_s and β_s. A review of the threeprevious measurements of this process [8–10] can be found in Ref. [1]. Prior to our measurement, the database consisted of 29 points between 49 and 95 MeV. The best extant chiral effective field theory (χEFT) calculation [1] fits these data with a χ^2 per degree of freedom (χ^2/DOF) of 0.97 and gives (in units of 10^{-4} fm^3, used throughout)

$$\alpha_s - \beta_s = 7.3 \pm 1.8(\text{stat}) \pm 0.8(\text{th}). \quad (1)$$

Here, the Baldin sum rule (BSR) [11], a variant of the optical theorem, was used to constrain the fit. Evaluating the sum rule using proton photoabsorption cross-section data gives $\alpha_p + \beta_p = 13.8 \pm 0.4$ [12]. For the neutron, the requisite cross sections are found from empirical partial-wave amplitudes for pion photoproduction. We take $\alpha_n + \beta_n = 15.2 \pm 0.4$ [13] with the uncertainty highly correlated with that for the proton, and so

$$\alpha_s + \beta_s = 14.5 \pm 0.4. \quad (2)$$

This world database of deuteron Compton scattering is much smaller, is of poorer quality, and spans a narrower energy range than that for the proton. A statistically consistent proton Compton database up to 170 MeV contains 147 points [14], with its most recent χEFT fit of

$$\alpha_p = 10.65 \pm 0.35(\text{stat}) \pm 0.2(\text{BSR}) \pm 0.3(\text{th}),$$
$$\beta_p = 3.15 \mp 0.35(\text{stat}) \pm 0.2(\text{BSR}) \mp 0.3(\text{th}), \quad (3)$$

using the proton BSR. Combining Eqs. (1), (2), and (3) yields

$$\alpha_n = 11.1 \pm 1.8(\text{stat}) \pm 0.2(\text{BSR}) \pm 0.8(\text{th}),$$
$$\beta_n = 4.1 \mp 1.8(\text{stat}) \pm 0.2(\text{BSR}) \mp 0.8(\text{th}). \quad (4)$$

These numbers are consistent with an extraction of neutron polarizabilities from seven data points on $^2\text{H}(\gamma,\gamma' n)p$, taken on the quasielastic ridge above 200 MeV [15]. Again using the neutron BSR constraint, this gives

$$\alpha_n = 12.5 \pm 1.8(\text{stat})^{+1.1}_{-0.6}(\text{sys}) \pm 1.1(\text{th}),$$
$$\beta_n = 2.7 \mp 1.8(\text{stat})^{+0.6}_{-1.1}(\text{sys}) \mp 1.1(\text{th}), \quad (5)$$

where the theory uncertainty may be underestimated [16].

As the statistical uncertainties dominate the overall uncertainty in Eq. (1), there is a pressing need for more and better deuteron Compton data. In this Letter, we report a new and comprehensive measurement of the differential cross section for elastic Compton scattering from deuterium performed at the MAX IV Laboratory [17,18] in Lund, Sweden. This measurement nearly doubles the number of data points in the world database and enables us to extract α_n and β_n with statistical uncertainties that are substantially reduced compared to those of Eq. (4).

At the Tagged-Photon Facility [19,20] at the MAX IV Laboratory, we used a 15 nA, 45% duty factor pulse-stretched electron beam [21] with energies of 144 and 165 MeV to produce quasimonoenergetic photons in the energy range 65–115 MeV via the bremsstrahlung-tagging technique [22,23]. This range covers most previous experiments and extends the range towards higher energies by 20 MeV. The postbremsstrahlung electrons were momentum analyzed in a magnetic spectrometer and detected in a 62-channel scintillator hodoscope [24] located along the focal plane (FP). The resulting tagged-photon beam had an energy resolution of ~500 keV per channel and a mean flux of $\sim 2 \times 10^6$ MeV^{-1} s^{-1}. The collimated photon beam was incident on a scattering chamber containing liquid deuterium in a cylindrical cell (length 170 mm and diameter 68 mm) made from 120 μm Kapton foil. The thickness of the target was $(8.10 \pm 0.20) \times 10^{23}$ nuclei/cm^2. The average loss of incident-beam photons due to absorption in the target was approximately 2%. The tagging efficiency [23] was the ratio of the number of tagged photons that survived the collimation and struck the target to the number of postbremsstrahlung electrons that were registered by the associated FP channel. It was monitored on a daily basis using a very low-intensity beam and a Pb-glass detector with 100% efficiency for the photons of interest. The tagging efficiency was determined to be $(44 \pm 1_{\text{sys}})\%$.

Three large-volume, segmented NaI(Tl) detectors [25–27] were used to detect the Compton-scattered photons. The detectors were each composed of a single, large NaI(Tl) core crystal surrounded by optically isolated, annular NaI(Tl) segments. The detectors had an energy resolution of better than 2% FWHM at energies near 100 MeV, which enabled the separation of elastically scattered events from events due to deuterium breakup. The signals from the NaI(Tl) detectors were passed to charge-integrating analog-to-digital converters (QDCs) and time-to-digital converters (TDCs) and the data were recorded on an event-by-event basis. The QDCs allowed reconstruction of the scattered-photon energies, while the TDCs provided the time correlation between the NaI(Tl) detectors and the FP hodoscope. The data-acquisition system was triggered by an event in any one of the NaI(Tl) detectors, which gated the QDCs and started the TDCs used for the timing measurements. The TDC stop signals came from the FP detectors. The energy calibration of each detector was determined by placing it directly into a low-intensity photon beam and observing the response as a function of tagged-photon energy. The energy calibration was confirmed to ~1% with the 131.4 MeV photon from the capture of π^-s on deuterium and reconstruction of the π^0 mass in back-to-back kinematics as defined by opposing NaI detectors.

In the scattering configuration, the detectors were located at laboratory angles of 60°, 120°, and 150° and at corresponding distances of 34.3, 41.8, and 91.5 cm from the target. Data were collected over two separate four-week run periods. Gain instabilities in the NaI(Tl) detectors were corrected using the location of the QDC peak for selected cosmic rays (those that pass through the diameter of the core crystal) on a run-by-run basis. Missing energy (ME) was defined as the difference between the energy registered in the NaI(Tl) detector and the tagged-photon energy corrected for the Compton scattering energy shift. GEANT4 [28] simulations of the detector line shapes were empirically broadened to match the measured in-beam detector responses. Scattering-configuration GEANT4 simulations of the *in situ* detector responses, acceptances, and efficiencies were based on the broadened in-beam results and were used to determine the total yield in the elastic-scattering peak. The sum of the resulting GEANT4 line shape and an accidental background was fit to the data. The GEANT4 simulation was also used to correct for the detection efficiency of the NaI(Tl) detector over a region of interest (ROI) of $-2.0 < \text{ME} < 2.0$ MeV, the ME

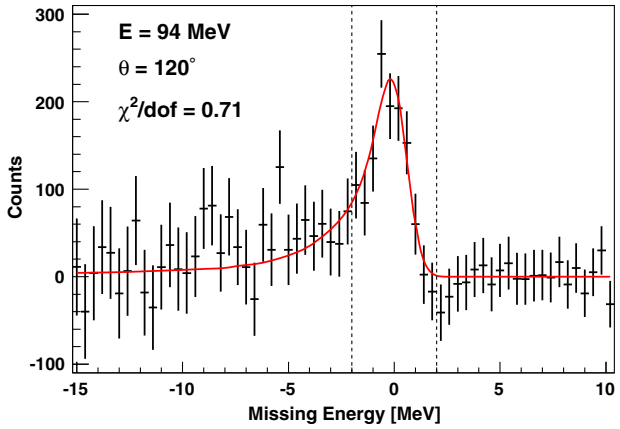

FIG. 1 (color online). A typical accidental-corrected scattered-photon spectrum together with a simulation (red) of the response function of the detector. The vertical, dashed lines indicate the $-2.0 < \mathrm{ME} < 2.0$ MeV yield-integration region.

integration region used to determined the yield. The ROI was dictated by the resolution of the detectors and the 2.2 MeVthreshold for the breakup of deuterium. The fitting procedure was repeated with a second line shape that simulated photons from $^2\mathrm{H}(\gamma,\gamma')np$. The contribution of these photons to the extracted yield in the ROI was consistent with zero. Additionally, extraction of the cross section for a slightly wider or narrower ROI produced results in agreement with those presented here. Effects associated with the finite size of the experimental apparatus as well as a correction for scattered photons absorbed by the target (∼1%) were also simulated. A typical accidental-corrected scattered-photon spectrum, the GEANT4 simulation of the response function of the detector, and the integration region are shown in Fig. 1. The simulation is clearly in good agreement with the data over the ROI ($\chi^2/\mathrm{DOF} = 0.71$).

The integrated scattered-photon yield was normalized to the number of photons incident on the target and corrected for rate-dependent factors [29], which were due to the physical overlap of the FP counters. This procedure has been systematically verified in measurements of photon scattering from carbon [30,31]. The number of photons incident on the target was determined from the number of postbremsstrahlung electrons detected in each FP channel, the tagging efficiency, and the rate-dependent correction factors.

The correlated systematic uncertainties for the experiment arise from the tagging efficiency (1%), target thickness (3%), target-cell contributions (3%), and rate-dependent effects (4%). Angle-dependent effects are the product of the solid angle and detection efficiency (3% at 150° and 4.2% otherwise). Point-to-point systematic uncertainties are dominated by the yield extraction (∼5%). A detailed discussion of the uncertainties, as well as the cross sections, can be found in Ref. [32]. For the first data-production run, correlated systematic uncertainties add in quadrature to 5.2%, and for the second run, they add to 4.7%. A table of cross sections is provided in the Supplemental Material [33].

The extraction of α_s and β_s from deuteron Compton scattering cross sections is not straightforward. Even for the case of the proton, most of the world data is beyond the energy at which a low-energy expansion of the cross section is valid. At energies above 100 MeV, the energy-dependent effects of the pion cloud and of the $\Delta(1232)$ excitation become important. Furthermore, the response of the deuteron to electric and magnetic fields is not just that of the constituent proton and neutron; for instance, pion-exchange currents contribute a substantial fraction of the deuteron Compton cross section at these energies [34]. χEFT is ideally suited to account consistently for both these aspects since it encodes the correct symmetries and degrees of freedom of QCD in model-independent Compton-scattering amplitudes with systematically improvable theoretical uncertainties. It predicts the full energy dependence of the single-nucleon scattering response (including spin-dependent amplitudes). For the deuteron, it consistently accounts for nuclear binding and obtains the correct Thomson limit by including NN rescattering [35].

Here, we summarize the ingredients of our recent χEFT analysis at order $e^2\delta^3$ (next-to-leading order in α and β), as detailed in Sec. 5.3 of Ref. [1]. The degrees of freedom are point nucleons with anomalous magnetic moments, a dynamical $\Delta(1232)$, treated nonrelativistically and without width, and the chiral pion clouds of both the proton and $\Delta(1232)$ at their respective leading orders. Two short-distance contributions to α_s and β_s are the only free parameters in our theory, since the $\gamma N\Delta$ $M1$ coupling is determined from proton Compton scattering. We compute the photon-deuteron scattering amplitude to $O(e^2\delta^3)$, and so include all these one- and two-nucleon effects. The dependence of our results on the deuteron wave function and NN potential is negligible.

We now fit α_s and β_s using this theory. We use the same fit procedure and parameters as in Ref. [1] and further details will appear in an upcoming publication [36]. Our fit adds point-to-point and angle-dependent systematic uncertainties in quadrature to the statistical uncertainty, and subsumes overall systematic uncertainties into a floating normalization [see Eq. (4.19) of Ref. [1] and references therein]. The deuteron Compton database of Ref. [1] is augmented by the two experimental runs reported here, which are treated as separate data sets with independent floating normalizations. Treating them as one single data set does not significantly affect the results. The theoretical uncertainty in the extracted polarizabilities from contributions beyond chiral order $e^2\delta^3$ has been assessed as ± 0.8 [1].

Within the statistical uncertainties, consistent results are obtained whether we analyze the new data alone, or in conjunction with the previous world data. Here, we present results only for the latter. In either case, the total χ^2 receives an unacceptably large contribution from two

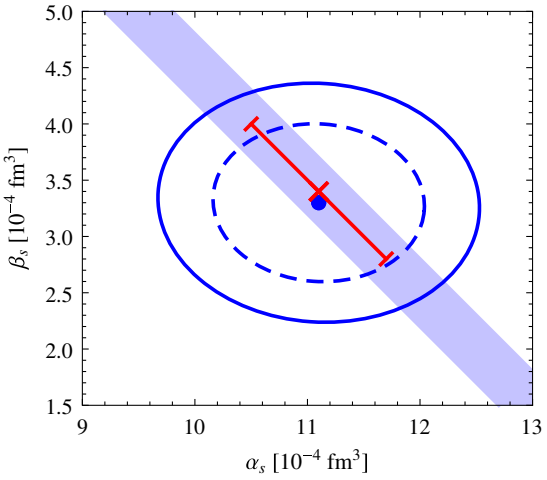

FIG. 2 (color online). The 1σ ($\chi^2 + 2.3$, solid ellipse) and $\chi^2 + 1$ (dashed ellipse) regions of the free fit compared to the Baldin-constrained fit (line); gray band: BSR.

points: 94.5 MeV, 60° and 112.1 MeV, 120°. These individually contribute at least 8.4 and 10.8 to the total χ^2, respectively (the exact contributions depend partially on fit details). The next largest contribution from a single datum is less than 4.6. Standard hypothesis-testing techniques thus require these two points to be excluded if the data set is to be statistically consistent. Fitting both the polarizabilities, we find

$$\alpha_s = 11.1 \pm 0.9(\text{stat}) \pm 0.8(\text{th}),$$
$$\beta_s = 3.3 \pm 0.6(\text{stat}) \pm 0.8(\text{th}), \quad (6)$$

with $\chi^2 = 49.2$ for 43 degrees of freedom. This is in very close agreement with the isoscalar BSR [Eq. (2)], which we can therefore use to reduce the statistical uncertainties. We then find

$$\alpha_s - \beta_s = 7.8 \pm 1.2(\text{stat}) \pm 0.8(\text{th}), \quad (7)$$

which agrees well with Eq. (1). This result leads to

$$\alpha_s = 11.1 \pm 0.6(\text{stat}) \pm 0.2(\text{BSR}) \pm 0.8(\text{th}),$$
$$\beta_s = 3.4 \mp 0.6(\text{stat}) \pm 0.2(\text{BSR}) \mp 0.8(\text{th}). \quad (8)$$

The total χ^2 is now 45.2 for 44 degrees of freedom. If we were to reinstate the two outliers, the central values would be 11.5 and 3.0, with $\chi^2 = 70.2$. We emphasize that the new data decrease the statistical uncertainty by 33%. We observe that the overall normalization of each data set floats by less than 5%, indicating good absolute cross-section normalizations. The χ^2/DOF of previous sets barely changes when the new data are added. Further details will be given in Ref. [36]. Figure 2 shows the 1σ ellipses of the free and Baldin-constrained fits. Cross sections and fits are shown in Fig. 3.

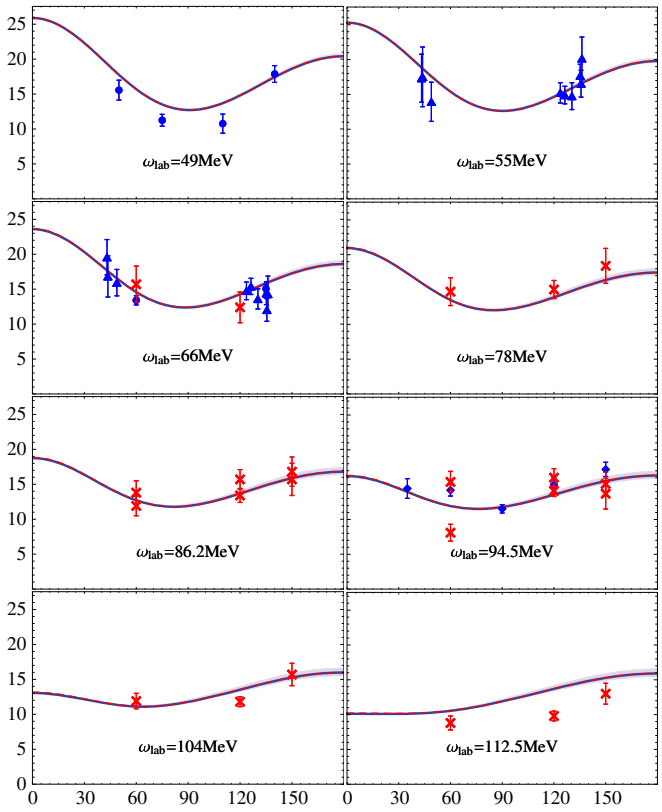

FIG. 3 (color online). Deuteron Compton scattering cross sections (in nb/sr) in the lab frame as a function of lab angle (in degrees). Data are within 2 MeV of the nominal energy. Data and statistical uncertainties: this work ×, Ref. [8] •, Ref. [9] ⧫, Ref. [10] ▲. Curves: results of the one (two) parameter fits [solid (dashed)]. Band: statistical uncertainty of the one-parameter fit. Note that the two points with $\Delta\chi^2 > 5$ are not included in the fit, and the normalization of each data set is floated within quoted uncertainties. See text for details.

In order to extract neutron polarizabilities, we combine the isoscalar values with the proton polarizabilities from Eq. (3) to obtain

$$\alpha_n = 11.55 \pm 1.25(\text{stat}) \pm 0.2(\text{BSR}) \pm 0.8(\text{th}),$$
$$\beta_n = 3.65 \mp 1.25(\text{stat}) \pm 0.2(\text{BSR}) \mp 0.8(\text{th}). \quad (9)$$

The shift in the central values from the previous extraction (4) is statistically insignificant, but our data shrink the statistical uncertainty by 30%. The result is in good agreement with that from quasielastic scattering (5).

The BSR determinations of the proton and neutron $\alpha + \beta$ provide evidence for an isovector component of the sum of polarizabilities of around 10% of the isoscalar part. In contrast, the present statistical and theoretical uncertainties on $\alpha - \beta$ are much too large to detect a significant proton-neutron difference. The forthcoming extension of the higher-order χEFT calculation on the proton [14] to the deuteron should reduce the theory uncertainty substantially. However, the statistical uncertainty still dominates, so there

is still a need for additional high-accuracy deuteron data. Experiments are ongoing or planned at MAMI [37], the MAX IV Laboratory, and HIγS [38]. This continued effort to illuminate the structure of the nucleon through Compton-scattering measurements should soon directly confront lattice QCD extractions of α and β.

Here, we have reported on an important step in this direction. Differential cross sections for elastic scattering from ^{2}H have been measured using quasimonoenergetic tagged photons with energies in the range 65–115 MeV at laboratory angles of 60°, 120°, and 150° at the Tagged-Photon Facility at the MAX IV Laboratory in Lund, Sweden. These data were used to extract the isoscalar polarizabilities and reduced the statistical uncertainty on these quantities by 33%, thereby appreciably tightening the constraints on neutron structure from Compton scattering.

The authors acknowledge the support of the staff of the MAX IV Laboratory. We also acknowledge the Data Management and Software Centre, a Danish contribution to the European Spallation Source ESS AB, for providing access to their computations cluster. We are grateful to the organizers and participants of the workshops Compton Scattering Off Protons and Light Nuclei: Pinning Down the Nucleon Polarizabilities, ECT$*$, Trento (Italy, 2013), and Bound States and Resonances in Effective Field Theories and Lattice QCD Calculations, Benasque (Spain, 2014). The Lund group acknowledges the financial support of the Swedish Research Council, the Knut and Alice Wallenberg Foundation, the Crafoord Foundation, the Swedish Institute, the Wenner-Gren Foundation, and the Royal Swedish Academy of Sciences. This material is based upon work supported by the National Science Foundation under Grant No. 0855569; the U.S. Department of Energy, Office of Science, Office of Nuclear Physics under Awards No. DE-FG02-93ER40756, No. DE-FG02-95ER40907, and No. DE-FG02-06ER41422; and the UK Science and Technology Facilities Council under Grants No. ST/F012047/1 and No. ST/J000159/1.

[*]Present address: Thomas Jefferson National Accelerator Facility, Newport News, Virginia 23606, USA.
[†]Corresponding author.
kevin.fissum@nuclear.lu.se
[‡]Present address: National Security Technologies, Andrews Air Force Base, Maryland 20762, USA.
[§]Present address: Pacific Northwest National Laboratory, Richland, Washington 99352, USA.

[1] H. W. Grießhammer, J. A. McGovern, D. R. Phillips, and G. Feldman, Prog. Part. Nucl. Phys. **67**, 841 (2012).
[2] H. W. Grießhammer, A. L. L'vov, J. A. McGovern, V. Pascalutsa, B. Pasquini, and D. R. Phillips, arXiv:1409.1512.
[3] M. Lujan, A. Alexandru, W. Freeman, and F. X. Lee, Phys. Rev. D **89**, 074506 (2014); W. Detmold, B. Tiburzi, and A. Walker-Loud, AIP Conf. Proc. **1441**, 165 (2012).
[4] K. Pachucki, Phys. Rev. A **60**, 3593 (1999).
[5] C. E. Carlson and M. Vanderhaeghen, arXiv:1109.3779.
[6] M. C. Birse and J. A. McGovern, Eur. Phys. J. A **48**, 120 (2012).
[7] A. Walker-Loud, C. E. Carlson, and G. A. Miller, Phys. Rev. Lett. **108**, 232301 (2012).
[8] M. A. Lucas, Ph.D. thesis, University of Illinois at Urbana-Champaign, 1994.
[9] D. L. Hornidge, B. J. Warkentin, R. Igarashi, J. C. Bergstrom, E. L. Hallin, N. R. Kolb, R. E. Pywell, D. M. Skopik, J. M. Vogt, and G. Feldman, Phys. Rev. Lett. **84**, 2334 (2000).
[10] M. Lundin *et al.*, Phys. Rev. Lett. **90**, 192501 (2003).
[11] A. M. Baldin, Nucl. Phys. **18**, 310 (1960).
[12] V. Olmos de León *et al.*, Eur. Phys. J. A **10**, 207 (2001).
[13] M. I. Levchuk and A. I. L'vov, Nucl. Phys. **A674**, 449 (2000).
[14] J. A. McGovern, D. R. Phillips, and H. W. Grießhammer, Eur. Phys. J. A **49**, 12 (2013).
[15] K. Kossert *et al.*, Eur. Phys. J. A **16**, 259 (2003).
[16] A. I. L'vov (private communication).
[17] https://www.maxlab.lu.se.
[18] M. Eriksson, in *Proceedings of IPAC, Dresden, Germany, 2014* [Joint Accelerator Conferences Website (JACoW), Geneva, Switzerland, 2014], p. 2852, ISBN 978-3-95450-132-8 (http://accelconf.web.cern.ch/AccelConf/IPAC2014/papers/thppa03.pdf).
[19] https://www.maxlab.lu.se/node/1090.
[20] J.-O. Adler *et al.*, Nucl. Instrum. Methods Phys. Res., Sect. A **715**, 1 (2013).
[21] L.-J. Lindgren, Nucl. Instrum. Methods Phys. Res., Sect. A **492**, 299 (2002).
[22] J.-O. Adler, B.-E. Andersson, K. I. Blomqvist, B. Forkman, K. Hansen, L. Isaksson, K. Lindgren, D. Nilsson, A. Sandell, B. Schröder, and K. Ziakas, Nucl. Instrum. Methods Phys. Res., Sect. A **294**, 15 (1990).
[23] J.-O. Adler, B.-E. Andersson, K. I. Blomqvist, K. G. Fissum, K. Hansen, L. Isaksson, B. Nilsson, D. Nilsson, H. Ruijter, A. Sandell, B. Schröder, and D. A. Sims, Nucl. Instrum. Methods Phys. Res., Sect. A **388**, 17 (1997).
[24] J. M. Vogt, R. E. Pywell, D. M. Skopik, E. L. Hallin, J. C. Bergstrom, H. S. Caplan, K. I. Blomqvist, W. D. Bianco, and J. W. Jury, Nucl. Instrum. Methods Phys. Res., Sect. A **324**, 198 (1993).
[25] J. P. Miller, E. J. Austin, E. C. Booth, K. P. Gall, E. K. McIntyre, and D. A. Whitehouse, Nucl. Instrum. Methods Phys. Res., Sect. A **270**, 431 (1988).
[26] F. Wissmann *et al.*, Nucl. Phys. **A660**, 232 (1999).
[27] L. S. Myers, Ph.D. thesis, University of Illinois at Urbana-Champaign, 2010.
[28] S. Agostinelli, Nucl. Instrum. Methods Phys. Res., Sect. A **506**, 250 (2003).
[29] L. S. Myers, G. Feldman, K. G. Fissum, L. Isaksson, M. A. Kovash, A. M. Nathan, R. E. Pywell, and B. Schröder, Nucl. Instrum. Methods Phys. Res., Sect. A **729**, 707 (2013).
[30] L. S. Myers *et al.*, Phys. Rev. C **89**, 035202 (2014).
[31] M. F. Preston, L. S. Myers, J. R. M. Annand, K. G. Fissum, K. Hansen, L. Isaksson, R. Jebali, and M. Lundin, Nucl. Instrum. Methods Phys. Res., Sect. A **744**, 17 (2014).

[32] L. S. Myers, J. R. M. Annand, J. Brudvik, G. Feldman, K. G. Fissum, K. Hansen, H. W. Grießhammer, S. S. Henshaw, L. Isaksson, R. Jebali, M. A. Kovash, M. Lundin, D. G. Middleton, A. M. Nathan, B. Schröder, and S. C. Stave (to be published).

[33] See Supplemental Material at http://link.aps.org/supplemental/10.1103/PhysRevLett.113.262506 for a table of measured cross sections.

[34] S. R. Beane, M. Malheiro, D. R. Phillips, and U. van Kolck, Nucl. Phys. **A656**, 367 (1999).

[35] R. P. Hildebrandt, H. W. Grießhammer, and T. R. Hemmert, Eur. Phys. J. A **46**, 111 (2010).

[36] H. W. Grießhammer, J. A. McGovern, and D. R. Phillips (to be published).

[37] J. R. M. Annand *et al.*, "Proposal for MAMI-A2-01-2013: Compton Scattering on the He Isotopes with an Active Target" (unpublished).

[38] H. R. Weller, M. W. Ahmed, H. Gao, W. Tornow, Y. K. Wu, M. Gai, and R. Miskimen, Prog. Part. Nucl. Phys. **62**, 257 (2009).